Progress In Electromagnetics Research, PIER 70, 175–189, 2007

MODAL ANALYSIS OF AZIMUTHALLY PERIODIC VANE-LOADED CYLINDRICAL WAVEGUIDE INTERACTION STRUCTURE FOR GYRO-TWT

G. Singh

Department of Electronics and Communication Engineering
Jaypee University of Information Technology
Solan-173 215, India

B. N. Basu

Department of Electronics Engineering
Institute of Technology
Banaras Hindu University
Varanasi-210 005, India

Abstract—This article discusses the gain-frequency characteristics of most competing modes of azimuthally periodic vane-loaded cylindrical waveguide interaction structure for gyrotron traveling wave tube (gyro-TWT) amplifier, which is the device of increasing importance because of its high-power and broad bandwidth capabilities. Vane-loading is identified as a means to achieve a low-beam energy, high-harmonic, low-magnetic field, mode-selective and stable operation of a gyro-TWT, and thus the development of a simple approach to the analysis of a vane-loaded gyro-TWT have been identified as a problem of practical relevance.

1. INTRODUCTION

The growth of satellite-based digital communications system over the past decade has opened lucrative commercial opportunities for vacuum electronic devices. This exciting new area requires the efficient production of high frequency power and ability to handle spectrally efficient modulations within stringent packing constraints at affordable cost. Commercial satellite communication systems, broadcasting, industrial heating, and air traffic control radar also rely heavily on vacuum electron devices for reliable performance at high power

and high efficiency. The military has critical reliance on vacuum sources for radar, electronic warfare, and satellite communications system requiring high-power, high-efficiency at high- frequency. The existing possibilities opened up by new design tools, approaches, and electromagnetic structures will yield a continuing stream of revolutionary advances in RF vacuum tube technology. Thus, the operational demand on RF systems to achieve greater functionality, scientific innovation driven by technical opportunity and market demand have been and continue to be the major forces behind the growth in the development of vacuum electronic devices. In the area of sources for high-resolution radar and high-information density communication systems the gyrotron traveling wave tube (gyro-TWT) amplifiers are most significant device [1–5]. The work is now progress to improve the average as well as peak power of gyro-TWT amplifiers at millimeter wave frequencies in order to build tubes suitable for use in future advanced radar systems, and there will probably be an attempt to improve the bandwidth beyond one 1 GHz. The continued development of important related technologies and advanced materials will continue to contribute to the range of capabilities and applications for the gyro-TWT's.

The gyro-TWT is an efficient high-power microwave and millimeter wave coherent radiation source of the gyro-device family, based on the electron cyclotron maser instability and configured as an amplifier [1–26]. It uses a non-resonant RF interaction structure, namely, a waveguide, to support a travelling wave for distributed interaction. Obviously, the gyro-TWT (in a non-resonant structure) has a better wideband amplification potential than a gyro-klystron (in a resonant structure) [1–5]. The benefit of the gyro-devices is derived from the combination of cyclotron resonance interaction and the fast wave interaction circuits. In the fast wave interaction circuits [27] the electric field strength can be quite high, independent of the proximity of the metallic circuit structure. This enables the electron beam to be situated in regions of high-electric field (to produce optimum coupling) without placing the beam in close proximity to delicate circuit structures. The axial phase synchronism takes between the electrons gyrating in helical paths and a co-propagating travelling RF wave. The electrons moving in helical paths under the influence of the modulating RF electric field form into a bunch (relativistic azimuthal) that twists around the helix system with a pitch substantially greater than the electron pitch [5]. The helical electron trajectories for a gyro-TWT can be formed by an MIG (magnetron injection gun). The electrons in helical trajectories with rotational energies take part in cyclotron-resonance interaction with the transverse RF electric field

in the waveguide and the required DC background magnetic field for this purpose is provided by the main solenoid. The spatial positions where electrons in the bunch are decelerated advances with a phase velocity approximately equal to the phase velocity of the RF wave in the waveguide. This process yields a continuous interaction and energy transfer from the phase modulated electrons to the RF wave over a relatively long length of the interaction structure along which the RF wave grows exponentially. At large interaction lengths near the exit of the interaction structure, spatial growth rate of RF waves saturates due to nonlinear effects. The beam after it takes part in interaction enters a magnetic decompression region and diverges off the axis to settle on the surface of the collector surrounding the beam [2–24]. The RF output is coupled out from a region further down the axis of the tube beyond an output window, which is vacuum-sealed to the tube. The output coupling arrangement has also to provide for the necessary waveguide-mode conversion since the mode of the waveguide interaction structure could, in general, be different from that of the output waveguide system.

This paper is organized as follows. The Section 2 discusses the motivation to take the vane-loaded cylindrical waveguide as interaction structure for gyro-TWT. The Section 3 describes the dispersion relation and small-signal gain of the vane-loaded gyro-TWT in brief because details are available in literature [18, 25]. The Section 4 concerned with the beam-wave interaction mechanism in the interaction structure. In the Section 5, result of the analysis is discussed. Finally, Section 6 concluded the analysis and explores the future scope of the work.

2. MOTIVATION

Experiments on gyro-TWTs are some aimed at achieving high powers, some wide bandwidths, some high gains, and some high efficiency, and, accordingly, the design considerations were made. For instance, if the gain is not the criterion, both axial tapering of the waveguide cross section and axial profiling of the magnetic field have increased the bandwidth of a gyro-TWT [3, 4, 17]. Similarly, for large gains, a resistive wall waveguide was used in order to stabilize the device against spurious oscillations [7–10] or use a number of stages with severs [16]. Furthermore, design considerations were made like reducing the required background magnetic field in the gyro-TWT experiment by operating the device at high cyclotron beam-harmonic resonance in a whispering gallery waveguide mode in the large-orbit configuration [8–10].

At beam energies considered practical for microwave devices, cyclotron interaction weakens rapidly as one increases the harmonic number for reducing the magnetic field requirement [4, 6, 8–19]. Moreover, at high harmonics severe mode competition occurs [12, 19, 22]. Thus, it appears that the successful operation of a high-harmonic gyro-TWT with low magnetic field requirement that can be operated with low-energy electron beams and with means for harmonic selection calls for some fundamental modification of the conventional smooth-wall waveguide configuration. As well as for optimum performance, the device should be designed such that the desired mode dominates and suppresses all other modes during the transition of the device parameters to the operating point. Such selective excitation of the desired mode is an extremely difficult problem due to the presence of many competing modes [3–13, 18]. Therefore, study of the start-up scenario in the design of such a gyrotron amplifier operating at high-order modes is extremely important.

A cylindrical waveguide provided with wedge-shaped metal vanes projecting radially inward from the wall of the guide provides a structure configuration that can build up a gyro-TWT with low energy beam and low magnetic field with good mode selectivity [6, 11–19]. The vanes, arranged at a regular angular interval around the wall of the cylindrical waveguide as shown in Fig. 1, vanes create a periodic fringe field near the axis-circling electrons thus enriching the harmonic contents of RF fields as experienced by the electrons. Thus, the harmonic coupling in a vane-loaded cylindrical waveguide is enhanced over that in a smooth-wall cylindrical waveguide. By adjusting the depth of the vanes one can position the fringe fields around electrons moving in small orbits of small Larmor radius. Moreover, if vanes are provided with the wall of the waveguide of a gyro-TWT in the large-orbit configuration [11–13, 18, 19], the radius of the beam of electrons circling the axis of the waveguide and interacting with the fringe field of the vanes could be reduced, that would in turn allow a reduction in beam energy. The vane-loaded structure also provides better mode selectivity in high harmonic operation [18, 19]. For high power gyro-TWT, the size of the waveguide is increased. An increase in the size of the waveguide reduces wall losses, but makes the resonator overmoded. Operating at a high beam harmonic requiring a reduced magnetic field, the vane-loaded gyro-TWT will also provide better mode selectivity and increased stability of the device as an amplifier. These advantages motivate to take the wedge-shape azimuthally periodic metal vane-loaded cylindrical waveguide as an interaction structure for gyro-travelling wave tube amplifier.

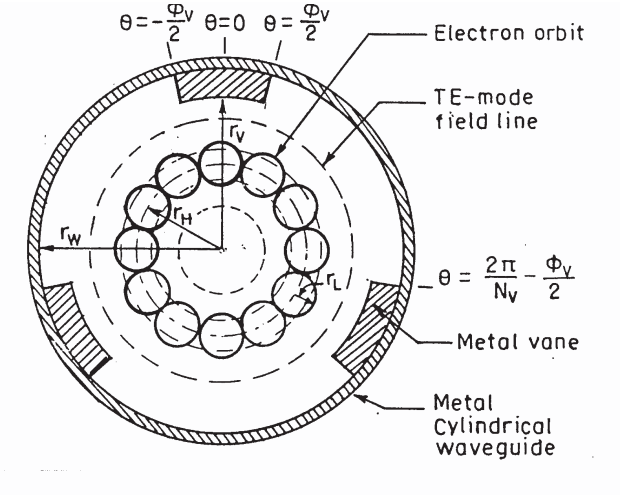

Figure 1. Transverse cross-section of small-orbit configuration of the vane-loaded cylindrical waveguide interaction structure of gyro-TWT.

3. INTERACTION STRUCTURE

We have taken an identical wedge-shaped azimuthally periodic metal vane-loaded cylindrical waveguide as an interaction structure for gyro-TWT and developed the cold (beam-absent) dispersion relation [18, 25, 26]. The periodicity of the vanes in the interaction structure generates the harmonic effects [25, 28]. The azimuthal harmonics effects arising from the angular periodicity of the vanes have been included in the field expressions. The dispersion relation of the vane-loaded cylindrical waveguide has been developed with the help of the field expressions and the relevant boundary conditions. The cold dispersion relation of the vane-loaded cylindrical waveguide interaction structure as shown in Fig. 1 for the $TE_{\nu n}$ mode is [14–19, 25, 26]:

$$\phi_V J'_\nu \{k_c r_V\} + (2\pi/N_V - \phi_V) \left[(1+\eta_\nu) J_\nu\{k_c r_V\} - \eta_\nu \left(J'_\nu \{k_c r_W\} / Y'_\nu \{k_c r_W\}\right) Y_\nu\{k_c r_V\}\right] = 0 \quad (1)$$

where η_ν is given by:

$$\eta_\nu = \frac{J'_\nu \{k_c r_V\} Y'_\nu \{k_c r_W\}}{J'_\nu \{k_c r_W\} Y'_\nu \{k_c r_V\} - J'_\nu \{k_c r_V\} Y'_\nu \{k_c r_W\}}.$$

where N_V is the number of metal vanes, each of angular thickness ϕ_V. r_V and r_W are the inner edge radius of vanes and waveguide

wall radius, respectively. J_ν and Y_ν are the νth order ordinary Bessel functions of first and second kind, respectively. The prime indicates the differentiation of the Bessel functions with respect to their arguments. Once the value of k_c is obtained from the solution of (1), one can find the axial phase propagation constant of the structure β from the general waveguide-mode relation: $k_0^2 - \beta^2 - k_c^2 = 0$, where k_0 $(= \omega/c)$ is the free-space propagation constant, ω being the wave angular frequency, and c the speed of light. For an even number of vanes, the vane-loaded cylindrical waveguide can support $N_V/2 + 1$ azimuthal modes, where N_V is the number of vanes. Each mode has characteristic phase shift between adjacent slots of $2m\pi/N_V$, where $m = 0, 1, 2, \ldots, N_V/2$ and is composed of infinite sum of $(m+kN_V)$th order azimuthal harmonics, where $k = 0, \pm1, \pm2, \ldots ..$ As in the magnetron, the modes of interest are the 2π mode $(m = 0)$, where the phase in each slot is identical, and the π mode $(m = N_V/2)$, where adjacent slots are out of phase by π [19]. For each mode, one may like to choose the vane number N_V such that the strongest non-zero azimuthal field harmonic coincides with the desired cyclotron harmonic number. The strength of interaction in a vane-loaded gyro-TWT, which depends on the energy stored per unit interaction length U_l, say, may be estimated by the interaction impedance of the structure. Since the interaction impedance is inversely proportional to U_l, and the vanes reduce RF fields in the outer region between vanes of the structure, the value of U_l is significantly reduced, and, consequently, that of the interaction impedance increased by the presence of vanes [9]. Also an expression for the azimuthal interaction impedance of the vane-loaded cylindrical waveguide is obtained, which measures the available azimuthal RF electric field for a given power propagating down the waveguide for electrons to interact with field [25]. Hence, the azimuthal interaction impedance preliminarily estimates the strength of beam-wave interaction in the device. One should not expect that the vane-loaded cylindrical waveguide, which is the azimuthally periodic, would have the shape of its dispersion characteristics changed by changing the vane parameters, unlike the axially periodic disc-loaded cylindrical waveguide. It will of interest to see the effects of varying the vane parameters, namely, number of vanes N_V, vane wedge angle ϕ_V, and vane tip radius r_V relative to waveguide-wall radius r_W on the shape of dispersion plots as well as on the cutoff frequency and interaction impedance which has already discussed [25].

The bean-present dispersion relation of the small-orbit gyro-TWT in a smooth-wall cylindrical waveguide for transverse electric mode at sth cyclotron harmonics has been derived in detail in the literature starting from the beam-present wave equation [14–19]. The dispersion

relation of the gyro-TWT can be interpreted to write the conventional TWT Pierce-type gain equation as:

$$G = A + BCN \tag{2}$$

where A and B are the launching loss and growth rate parameters, respectively. $N = \beta\ell/(2\pi)$ is the interaction length ℓ, expressed in terms of the number of the guide wavelengths. $C = (KI_0/4V_0)^{1/3}$, is the Pierce gain parameter, where I_0 and V_0 are the beam current and voltage, respectively. K, which has the dimension of the impedance, is identified as the interaction impedance of the gyro-TWT and defined as:

$$K = \frac{(\mu_0/\varepsilon_0)^{1/2}(v_t/c)^2 k_c^2(1+\alpha_0^2)J_{v-s}^2\{k_c r_H\}J_s'^2\{k_c r_L\}}{\pi r_W^2 \beta^4 (v_z/c)\left(1 - \dfrac{v^2}{k_c^2 r_W^2}\right) J_v^2\{k_c r_W\}} \tag{3}$$

where $\alpha_0(= v_t/v_z)$ is the beam velocity pitch factor. r_H and r_L are hollow beam radius and Larmor radius, respectively. v_t and v_z are transverse and axial velocity of the beam, respectively. The Pierce-type gain equation, which is valid for the gyro-TWT in a smooth-wall waveguide, is a function of Pierce parameter C. This Pierce parameter is proportional to the cube root of the interaction impedance K, which is also a function of the cold axial propagation constant β and cutoff wavenumber k_C of the waveguide [14–19]. The cold waveguide parameters, namely, the axial phase propagation constant and the cutoff wavenumber of the modes are obtainable from the solution of the cold dispersion relation (1) of the interaction structure. These parameters are plugged into the small-signal Pierce-type gain equation of a gyro-TWT in a smooth-wall waveguide for the evaluation of the interaction impedance (3) and hence the gain (2) of the vane-loaded gyro-TWT.

4. BEAM-WAVE INTERACTION

The small-orbit configuration of the device has been considered, which is rather general, since the analytical results of the large-orbit configuration easily follow, as a special case, from those of the small-orbit configuration, by taking the hollow-beam radius tending to zero [6, 8, 13, 19] and interpreting that the Larmor radius refers to the beam position as shown in Fig. 1. In a gyro-device, beam-wave interaction takes place between a cyclotron mode supported by the electron beam and a waveguide mode. The condition of synchronism between the

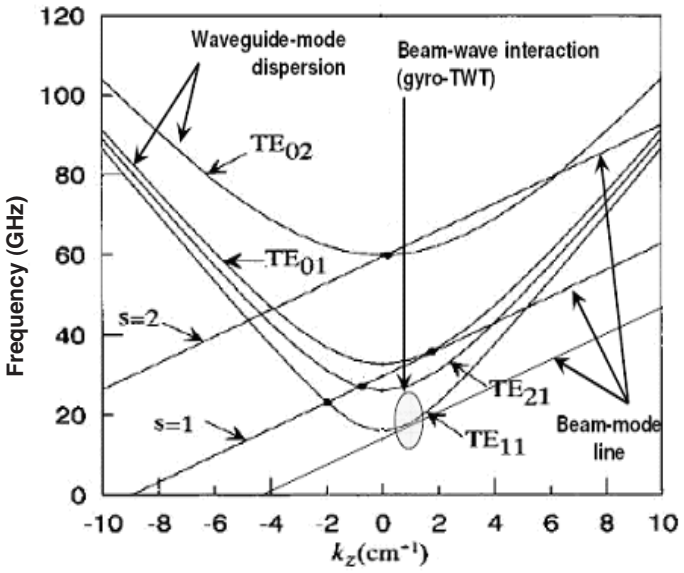

Figure 2. Dispersion characteristics of vane-loaded cylindrical waveguide interaction structure gyro-TWT. The typical structure parameters are: $N = 4$, $\phi = 45^\circ$ and $r_v/r_W = 0.6$.

transverse electronic motion and RF waves leads to the following beam-mode dispersion relation of a gyro-device [2–6]:

$$\omega - \beta v_z - s\omega_c/\gamma = 0 \tag{4}$$

where ω is the angular frequency of the RF wave, and β the axial phase propagation constant of the waveguide mode, v_z the axial electron velocity, s the beam-harmonic mode number. γ is relativistic mass factor. $\omega_c (= |e| B_0/m_{e0})$ is the non-relativistic cyclotron angular frequency, corresponding to the rest mass m_{e0} of an electron that carries a charge of e, with B_0 as the background magnetic flux density. The waveguide-mode dispersion relation is [4–19]:

$$\omega^2 - \beta^2 c^2 - \omega_{\text{cut}}^2 = 0 \tag{5}$$

where ω_{cut} is the angular cutoff frequency of the waveguide and c is the velocity of light. The $\omega - \beta$ plot of the beam-mode dispersion relation (4) is a straight line of slope equal to v_z, with $s\omega_c/\gamma$ as the intercept on the ω-axis. Similarly, the $\omega - \beta$ waveguide-mode dispersion plot, given by (5), is a hyperbola, with ω_{cut} as the intercept on the ω-axis as shown

in Fig. 2. If the beam-mode dispersion line intersects the waveguide-mode dispersion hyperbola, it should do so, in general, at two points, giving two possible operating points of a gyro device. A particular point of interest is the grazing intersection, when the beam-mode line barely touches or grazes the waveguide-mode hyperbola that is the point of interaction as shown in Fig. 2. At the grazing point, the slop of the hyperbola ($= d\omega/d\beta$), which also represent the group velocity of the wave, becomes equal to the slope of the beam-mode line, which is equal to the axial velocity v_z. The Doppler shift term βv_z in (4) is small resulting in radiation near the electron cyclotron or at one of its harmonics: $\omega \cong s\omega_c/\gamma$ (cyclotron harmonic resonance). The operating mode is chosen close to the cutoff (phase velocity $v_{ph}(= \omega/\beta) >> c$) (Fig. 2). A small, but positive, frequency mismatch ($= \omega - s\omega_c/\gamma$) ensures the achievement of the correct phasing to keep electron bunches in the retarding phase [5–8]. Harmonic operation ($\omega \cong s\omega_c/\gamma$) reduces ω_c and hence the required background magnetic flux density B_0 by a factor the of beam harmonic.

5. RESULTS

The results of cold analysis show no influence of changing vane parameters on the shape of the dispersion characteristics of a vane-loaded cylindrical waveguide. The waveguide cutoff frequency, however, significantly depends on the vane parameters [25]. The effects of varying the vane parameters, namely, the number of vanes, the angular vane width, and the vane tip radius relative to the radius of the waveguide on the value of the cutoff wave number of the waveguide as well as on the dispersion and azimuthal interaction impedance characteristics have been studied [25]. Earlier a study has been made on the optimizing role of the structure as well as beam and magnetic field parameters in maximizing the device gain [15–17]. Chong et al. [6] developed the cold analysis of a vane-loaded cylindrical waveguide for both π and 2π modes. In their cold analysis, azimuthal harmonics were considered in the vane-free region, while, in the region occupied by vanes, each vane was treated as a fundamental-mode rectangular waveguide with the electric field being solely azimuthal. Subsequently, in the analysis of the gyro-TWT they made the tenuous-beam approximation assuming that the beam does not perturb the mode profile so that the electron beam interacts with the RF field of an empty waveguide. They used the cold field solutions in a self-consistent code to investigate into the behaviour of a vane-loaded gyro-TWT. Shrivastava [20] also obtained a numerical boundary value, two region solution for fields in the vane-free and vane-occupied regions of

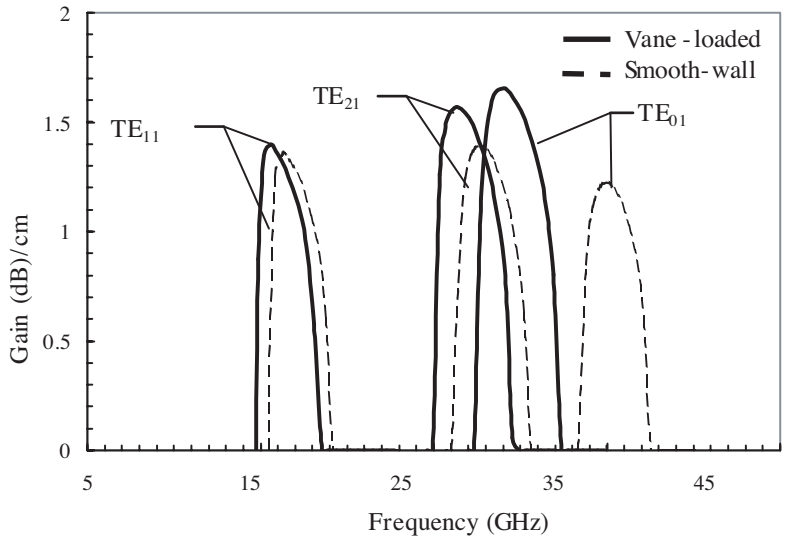

Figure 3. Optimized mode spectrum of vane-loaded gyro-TWT for TE_{01} ($m = 0,\ k = 0,\ n = 1$), TE_{11} ($m = 1,\ k = 0,\ n = 1$), and TE_{21} ($m = 2,\ k = 0,\ n = 1$). The typical interaction structure parameters are: $N = 4$, $\phi = 45^\circ$ and $r_v/r_W = 0.6$.

the vane-loaded cylindrical waveguide and determine the eigenvalue. In the present analysis authors have been considered in harmonic effects in both the vane-free and vane-occupied regions.

In order to study the modal response of the device, three basic kinds of modes have been considered: typically, TE_{21} ($m = 2$, $k = 0$, $n = 1$) in which the electric field lines are concentrated near the waveguide wall, TE_{01} ($m = 0$, $k = 0$, $n = 1$), in which the electric field lines circle around the waveguide axis with no azimuthal variation, and TE_{11} ($m = 1$, $k = 0$, $n = 1$) in which the electric field lines lie across the waveguide cross section. Out of these three modes, the TE_{21} mode enjoys the highest gain for relatively small hollow beam radii considered, requiring low-energy beams as shown in Fig. 3. The fringe field of the vanes alters the azimuthal electric field as well as the power propagating down the structure and hence the interaction impedance of the structure. With the introduction of vanes while the gains of the device in the TE_{01} and TE_{21} modes are much enhanced compared to that of smooth-wall waveguide, however, the gain in the TE_{11} mode is not much enhanced as TE_{01} and TE_{21} modes. The TE_{21}-mode gain is higher than the TE_{01}-mode gain, irrespective of whether the vanes are absent or present. The change in gain due to the introduction

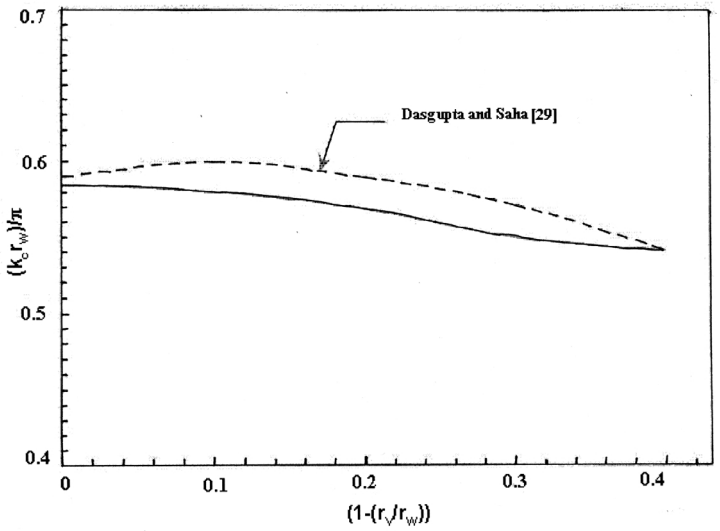

Figure 4. Eigenvalue of the vane-loaded cylindrical waveguide calculated for various vane-depths by the present analysis validated against by Ritz-Galerkin's technique due to Dasgupta and Saha [29] for TE_{11} mode over a range of vane-depth for typically, $N_V = 4$ and $\phi_V = 40°$.

of vanes is however found to be more for the TE_{01} mode than for the TE_{21} mode, despite the vanes affecting the field lines of the TE_{21} mode, which are closer to the waveguide wall with which the vanes are provided, more than the field lines of the TE_{01} mode, which are close to the waveguide axis. The reason could be that due to the introduction of vanes the field spreads in the azimuthal direction more for the TE_{01} mode than for the TE_{21} mode thus allowing the electrons to experience the azimuthal field over a greater orbital length for interaction in the TE_{01} mode than in the TE_{21} mode. Further, there exists an optimum beam radius corresponding to the maximum gain for the TE_{01} and TE_{21} modes, a behavior similar to what has been observed with respect to the value of the interaction impedance. With the introduction of vanes, gain-wise, the TE_{11} mode is well separated in the gain-frequency response as shown in Fig. 3. Moreover, at smaller beam radius, the vane-loaded device gives relatively large gain values, suggesting the possibility of realizing the device with low beam energies [18].

Mode-competition-wise, following the behaviour with respect to the cold dispersion characteristics as shown in Fig. 2, the gain-frequency characteristics of TE_{11} waveguide mode is found to be well separated in frequency from TE_{01} waveguide mode as well as from

TE_{21}, the later two being closely competitive to each other [15]. Thus, the mode competition behaviour with respect to cold dispersion characteristics has reflected on the gain-frequency response of the device, too. Finally, a attempts has made to validate the results obtained by authors present approach against the other obtained by Ritz-Galerkin's technique due to Dasgupta and Saha [29] for TE_{11} mode as shown in Fig. 4. The eigenvalue calculated by the present method has agreed for a small range of vane-depth. Recently, we have reported the validation of the results obtained by the present analysis of the interaction structure against those available in the literature typically, one by Shrivastava [20] for the TE_{21} mode for cold dispersion relation and other by Chong et al. [6] for the TE_{41} mode in the large-orbit configuration [18].

6. CONCLUSION

Due to strong interaction, one may expect to achieve large gains from a vane-loaded gyro-TWT, though not as wide bandwidths (because of narrow-band coalescence between the beam-mode and the waveguide-mode dispersion plots) as those obtainable from a gyro-TWT loaded with an axially periodic disc-loaded structure. The gain-frequency characteristics of TE_{11} waveguide mode is found to be well separated in frequency from TE_{01} waveguide mode as well as from TE_{21}, the later two being closely competitive to each other. The mode competition behaviour with respect to cold dispersion characteristics has also reflected on the gain-frequency response of the device. With a view to removing the narrow-band deficiency of the device, it will be of interest to analyze innovative device configurations, which combine the high-gain advantage of a vane-loaded gyro-TWT with any new schemes for broadbanding the device. In the family of gyro-devices, the gyro-TWT amplifier appears to be the most intricate, both in theory and experiment. Theoretical research led to the considerable physical insight into the principle of operation of a gyro-TWT. Certainly, in a vane-loaded gyro-TWT one finds a device having a gain higher than that of a gyro-TWT in a smooth-wall waveguide, which is controllable by vane parameters. Some of the mile-stones in the understanding of this principles are: the development of the single particle theory, the application of the kinetic theory for a planar configuration, the application of kinetic theory to the TE mode interaction in a cylindrical waveguide, the stability analysis, and the development of a non-linear self-consistent simulation code for the device in a rectangular or a cylindrical waveguide.

ACKNOWLEDGMENT

Authors are sincerely thankful to the reviewers for their critical comments and suggestions to improve the quality of the manuscript.

REFERENCES

1. Gaponov-Grekhov, A. V. and V. L. Granatstein (eds.), *Application of High Power Microwaves*, Artech House, Boston, 1994.
2. Felch, K. L., B. G. Danly, H. R. Jory, K. E. Kreischer, W. Lawson, B. Levush, and R. J. Temkin, "Characteristics and application of fast-wave gyro-devices," *Proc. IEEE*, Vol. 87, 752–781, 1999.
3. Chu, K. R., "Overview of research on the gyrotron traveling wave amplifier," *IEEE Trans. Plasma Sci.*, Vol. 30, 903–908, 2002.
4. Gold, S. H. and G. S. Nusinovich, "Review of high power microwave source research," *Rev. Sci., Instrum.*, Vol. 68, 3945–3974, 1997.
5. Chu, K. R., "The electron cyclotron maser," *Rev. Mod. Phys.*, Vol. 76, 489–540, 2004.
6. Chong, C. K., D. B. McDermott, A. T. Balkcum, and N. C. Luhmann, Jr., "Nonlinear analysis of high-harmonic slotted gyro-TWT amplifier," *IEEE Trans. Plasma Sci.*, Vol. 20, 176–187, 1992.
7. Denisov, G. G., V. L. Bratman, A. D. R. Phelps, and S. V. Samsonov, "Gyro-TWT with a helical operating waveguide: New possibilities to enhance efficiency and frequency bandwidth," *IEEE Trans. Plasma Sci.*, Vol. 26, 508–518, 1998.
8. Chong, C. K., D. B. McDermott, and N. C. Luhmann, "Large-signal operation of a third-harmonic slotted gyro-TWT amplifier," *IEEE Trans. Plasma Sci.*, Vol. 26, 500–507, 1998.
9. Chong, C. K., D. B. McDermott, A. T. Lin, W. J. DeHope, Q. S. Wang, and N. C. Luhmann, Jr., "Stability of a 95 GHz slotted third-harmonic gyro-TWT amplifier," *IEEE Trans. Plasma Sci.*, Vol. 24, 735–743, 1996.
10. McDermott, D. B., B. H. Deng, K. X. Liu, J. Van Meter, Q. S. Wang, and N. C. Luhmann, Jr., "Stable 2 MW, 35 GHz, third-harmonic TE_{41} gyro-TWT amplifier," *IEEE Trans. Plasma Sci.*, Vol. 26, 482–487, 1998.
11. Chu, K. R. and D. Dialetis, "Kinetic theory of harmonic gyrotron oscillation with slotted resonant structure," *Infrared and*

Millimeter Waves, Vol. 13, 45–75, Academic Press, New York, 1985.

12. Lau, Y. Y. and L. R. Barnett, "A low magnetic field gyrotron-gyro-magnetron," *Int. J. Electron.*, Vol. 53, 693–698, 1982.
13. Chong, C. K., D. B. McDermott, and N. C. Luhmann, Jr., "Slotted third harmonic gyro-TWT amplifier experiment," *IEEE Trans. Plasma Sci.*, Vol. 24, 727–734, 1996.
14. Singh, G., S. M. S. Ravi Chandra, P. V. Bhaskar, P. K. Jain, and B. N. Basu, "Control of the gain-frequency response of a vane-loaded gyro-TWT by beam and background magnetic field parameters," *Microwave and Optical Tech. Lett.*, Vol. 24, 140–145, 2000.
15. Singh, G., M. V. Kartikeyan, A. K. Sinha, and B. N. Basu, "Effects of beam and magnetic field parameters on highly competing TE_{01} and TE_{21} modes of vane-loaded gyro-TWT," *Int. J. Infrared and Millimeter Waves*, Vol. 23, 517–533, 2000.
16. Agrawal, M., G. Singh, P. K. Jain, and B. N. Basu, "Two-stage vane loading of gyro-TWT for high gains and bandwidths," *Microwave Optical and Technology Letters*, Vol. 27, No. 3, 210–213, 2000.
17. Agrawal, M., G. Singh, P. K. Jain, and B. N. Basu, "Analysis of tapered vane loaded broad band gyro-TWT," *IEEE Trans. Plasma Sci.*, Vol. 29, No. 3, 439–444, 2001.
18. Singh, G., S. M. S. Ravi Chandra, P. V. Bhaskar, P. K. Jain, and B. N. Basu, "Analysis of vane-loaded gyro-TWT for the gain-frequency response," *IEEE Trans. Plasma Sci.*, Vol. 32, No. 5, 2130–2138, 2004.
19. Singh, G., M. V. Kartikeyan, and B. N. Basu, "Gain-frequency response of nearby waveguide mode in vane-loaded gyro-TWTs," *IEEE Trans. Plasma Sci.*, Vol. 34, No. 3, 554–558, June 2006.
20. Grow, R. W. and U. A. Shrivastava, "Impedance calculation for travelling wave gyrotrons operating at harmonics of cyclotron frequency in magnetron type circuits," *Int. J. Electron.*, Vol. 53, 699–707, 1982.
21. McDermott, D. B., H. H. Song, Y. Hirata, A. T. Lin, T. H. Chang, H. L. Hsu, K. R. Chu, and N. C. Luhmann, Jr., "Design of a W-band TE_{01} mode gyrotron travelling wave amplifier with high-power and broadband capabilities," *IEEE Trans. Plasma Sci.*, Vol. 30, 894–902, 2002.
22. Wang, Q. S., C. S. kou, D. B. McDermott, A. T. Lin, K. R. Chu, and N. C. Luhmann, Jr., "High-power harmonic gyro-TWTs —

Part II: Nonlinear theory and design," *IEEE Trans. Plasma Sci.*, Vol. 20, 163–169, 1992.

23. Leou, K. C., D. B. McDermott, A. J. Balkcum, and N. C. Luhmann, Jr., "Stable high-power TE_{01} gyro-TWT amplifiers," *IEEE Trans. Plasma Sci.*, Vol. 22, 585–592, 1994.
24. Wang, Q. S., D. B. McDermott, and N. C. Luhmann, Jr., "Operation of a stable 200 kW second-harmonic gyro-TWT amplifier," *IEEE Trans. Plasma Sci.*, Vol. 24, 700–706, 1996.
25. Singh, G., S. M. S. Ravi Chandra, P. V. Bhaskar, P. K. Jain, and B. N. Basu, "Analysis of an azimuthally-periodic vane-loaded cylindrical waveguide for a gyro-travelling-wave tube," *Int. J. Electron.*, Vol. 86, 1463–1479, 1999.
26. Singh, K., P. K. Jain, and B. N. Basu, "Analysis of a coaxial waveguide corrugated with wedge-shaped radial vanes considering azimuthal harmonic effects," *Progress In Electromagnetics Research*, PIER 47, 297–312, 2004.
27. Ghosh, S., P. K. Jain, and B. N. Basu, "Fast-wave analysis of an inhomogeneously-loaded helix enclosed in a cylindrical waveguide," *Progress In Electromagnetics Research*, PIER 18, 19–43, 1998.
28. Lee, H. S., "Dispersion relation of corrugated circular waveguides," *Journal of Electromagnetic Waves and Applications*, Vol. 19, No. 10, 1391–1406, 2005.
29. Dasgupta, D. and P. K. Saha, "Modal properties of a quadruple-ridge circular waveguide by Galerkin's method," *Indian J. of Pure and Applied Physics*, Vol. 22, 106–109, 1984.